Hindawi Publishing Corporation
Journal of Nanomaterials
Volume 2011, Article ID 842613, 5 pages
doi:10.1155/2011/842613

Research Article

Biodistribution of ^{60}Co–Co/Graphitic-Shell Nanocrystals *In Vivo*

Li Zhan,[1] Qi Wei,[1] Geng Yanxia,[1] Xu Junzheng,[1] and Wu Wangsuo[1,2]

[1] *Radiochemistry Laboratory, School of Nuclera Science and Technology, Lanzhou University, Lanzhou 73000, China*
[2] *State Key Laboratory of Applied Organic Chemistry, Lanzhou University, Lanzhou 730000, China*

Correspondence should be addressed to Wu Wangsuo, wuws@lzu.edu.cn

Received 21 February 2011; Revised 12 April 2011; Accepted 23 May 2011

Academic Editor: Xing J. Liang

The magnetic nano-materials, Co/graphitic carbon- (GC-) shell nanocrystals, were made *via* chemicalvapour deposition (CVD) method, and their biodistribution and excretion in mice were studied by using postintravenously (i.v.) injecting with ^{60}Co–Co/GC nanocrystals. The results showed that about 5% of Co was embedded into graphitic carbon to form multilayer Co/GC nanocrystals and the size of the particle was ~20 nm, the thickness of the nanocrystal cover layer was ~4 nm, and the core size of Co was ~14 nm. Most of the nanocrystals were accumulated in lung, liver, and spleen after 6, 12, 18, and 24 h after *i.v.* with ^{60}Co–Co/GC nanocrystals. The nanoparticles were cleared rapidly from blood and closed to lower level in 10 min after injection. The ^{60}Co–Co/GC nanocrystals were eliminated slowly from body in 24 h after injection, ~6.09% of ^{60}Co–Co/GC nanocrystals were excreted by urine, ~1.85% by feces in 24 h, and the total excretion was less than 10%.

1. Introduction

Nanocrystals with advanced magnetics or optical properties has attracted increasing research interests in the past due to their potential biomedical applications such as bioseparation, biosensing, magnetic imaging, drug delivery, and magnetic fluid hyperthermia [1, 2]. Among various magnetic nanocrystals, cobalt is a class of ferromagnetic material with high magnetic moment density and is magnetically soft [3–6], but it has yet been explored owing to the problems of easy oxidation and potential toxicity. Previously, FeCo nanocrystals with multilayered graphitic carbon and pyrolytic carbon or inert metals have been obtained [6–8], and this nanomaterials seemed to be the best structure because of its high stability, low toxicity, and easy function alization up to now. Meanwhile, the single-shelled, discrete, chemically functionalized, and water-soluble forms, FeCo/GC nanocrystals, have been also developed for biological and medicinal applications in a recent work [9]. Therefore, researchers must investigate and improve further biocompatibility and biosafety before application *in vivo*, and then, it is important and necessary to study behavior and fate of pristine metals/GC nanocrystals *in vivo*. In order to detect simply and quantify accurately content of nanocrystals in various tissues, so radioactive isotopes were introduced into metals/GC nanocrystals, and which can be used as drug carrier and intermediate in radiation medicine fields. Thereby, as a new drug carrier with advanced magnetic and radioactive, it would be selectively localized to the target-site of tumor and focus by external magnetic field, and then, the drug and gamma ray would be delivered to cell and kill cancer cells or germ in future.

We developed a ^{60}Co–Co/GC nanocrystal with advanced magnetism and radioactivity, and the biodistribution and excretion of unfunctionalized ^{60}Co–Co/GC nanocrystals were investigated to research the behavior and fate *in vivo*, which will be important for researchers to devise and develop further functionalized, biosafe, and biocompatibly magnetic nanocrystals in clinical and radiation medicine.

2. Method and Materials

2.1. Synthesis of Co/GC Nanocrystals. According to the method of Seo et al. [9], we impregnated 1.00 g of fumed silica (Sigma) with 0.25 g $Co(NO_3)_2 \cdot 6H_2O$ in 50 mL ethanol and sonicated it for 1 h. After removal of ethanol and drying at 80°C, we ground the powder and typically used 0.50 g for methane CVD in a tube furnace. We heated the sample in H_2 flow to reach 800°C for 5 min and then subjected it

to methane flow of 600 cm^3 min^{-1} for 5 min. On cooling, we etched the sample with 10% HF in H_2O (80%) and ethanol (10%) to dissolve the silica. We collected the Co/GC nanocrystals by centrifugation and thoroughly washed them.

2.2. Characterization. We characterized the nanocrystals by TEM (JEM-2010, Nippon Tekno Co., Ltd.), Ramanspectroscopy (SPEX1403 micro-Raman spectrometer with a laser excitation of l = 785 nm, Spex Co., Ltd.), the elemental composition of nanocrystals was analyzed by Energy Dispersive Spectrdmeter (EDS, JEM-2010, Nippon Tekno Co., Ltd.).

2.3. Synthesis of ^{60}Co–Co/GC Nanocrystals. 1.74×10^8 cpm ^{60}Co–$Co(NO_3)_2$ solution was added into mixture suspension (1 g fumed silica and 0.25 g $Co(NO_3)_2 \cdot 6H_2O$ in 50 mL ethanol) and sonicated it for 1 h. Subsequently, the same synthesis method was operated to synthesize the ^{60}Co-Co/GC nanocrystals. The samples were centrifugated and washed thoroughly until supernatant fluid without radioactive counts. Finally, the yields of products were calculated as

$$y = \frac{C}{C_0} \times 100\% \quad (1)$$

y: yields of sample; C: radioactive counts in nanocrystals; C_0: radioactive counts in reactants.

2.4. Biodistribution and Excretion Study in Mice. The ^{60}Co–Co/GC nanocrystals were dispersed ultrasonically into PBS solution. Female Kongming White mice weighing 16–20 g were obtained from Laboratory Center for Medical Science, Lanzhou University, Gansu, China. Food and water were provided ad libitum throughout experimental period.

The five groups of mice (eight mice per group) were injected intravenously with 1.86×10^5 cpm/per mouse suspension of ^{60}Co–Co/GC nanocrystals. Five groups were sacrificed at 1, 6, 12, 18, and 24 h, respectively. Their tissues, including the heart, lung, liver, spleen, kidney, stomach, and intestine, were immediately dissected, and feces and urine were collected, respectively. Each tissue was wrapped in foil, weighted, and counted for ^{60}Co count. Distribution in tissues was presented in percent injected dose per gram of wet tissue (% ID/g), which could be calculated by the percent injected dose (tissue activity/total activity dosed) per gram of wet tissue. The excretion of ^{60}Co–Co/GC nanocrystals from mice was investigated by counting ^{60}Co in the urine and feces of mice at different time intervals from 0 to 24 h after dosing. Results were expressed as percent injected dose per gram of wet tissue.

2.5. Hemodynamics. Another nine groups mice (six mice/per group) were injected intravenously with 1.86×10^5 cpm/per mouse ^{60}Co–Co/GC nanocrystals to study hemodynamics, the nine groups were sacrificed at 0, 5, 10, 30, 40 min, 1 h, 6 h, 12 h, 18 h, and 24 h, respectively. 0.1 mL blood was collected immediately to count by gamma counter (BH-2001gamma spectrometry, CNNC).

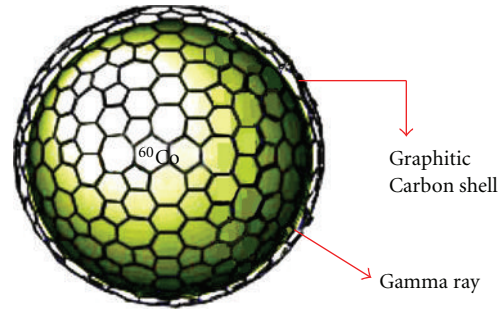

Figure 1: The schematic diagram of a ^{60}Co/GC nanocrystal. Note: the single carbon cage denotes the multilayer graphitic carbon shells.

3. Results and Discussion

3.1. Co/GC Nanocrystals. Co/GC nanocrystals have observed clearly from Figure 2, the TEM and HRTEM showed that the diameter of Co/GC nanocrystals was 20.46 ± 3.46 nm, the core diameter of Co nanocrystals was 13.77 ± 2.09 nm, and thickness of cover layer was 4.19 ± 0.82 nm. The elemental composition of nanocrystals were obtained by elemental analysis of EDS to show 25.73 of Co and 73.77% of C, and a little of O (0.33%) found may be from foreign matter such as ethanol or water (Figure 3). This indicated that Co and C in nanocrystals were existed as simple substances. Moreover, Raman spectroscopy was used to identify a graphitic carbon G peak at ~1,600 cm^{-1} and a disordered D peak at ~1,300 cm^{-1} (Figure 4), providing evidence for the graphitic shell [9, 10]. Therefore, the results showed that the multilayer Co/GC nanocrystals synthesized were much larger than FeCo/GC nanocrystals in previousreports [9]. Seo et al. have obtained single-layer FeCo/GC nanocrystals, and the diameter of FeCo/GC nanocrystals was smaller [9]. Meanwhile, they impregnated 1 g of fumed silica with different content of mixed metals salts to control diameter of nanocrystals. For example, for 7.2×10^{-4} mol mixed salts (Co/Fe = 3.6×10^{-4} mol), the size of FeCo/GC nanocrystals was ~7 nm, but for 1.8×10^{-4} mol mixed salts (Co/Fe = 0.9×10^{-4} mol), the size was ~4 nm [9]. In our work, we have selected only $Co(NO_3)_2$ to synthesize Co/GC nanocrystals according to the same method and condition with Seo et al. Therefore, as 8.60×10^{-4} mol Co used in reactants, the diameter of nanoparticles was ~20 nm, and the larger Co nanocrystals were embedded into thicker multilayer carbon shells. In other words, relative to Si identified with 1 g in reactants, with increasing of Co from 0.9, 3.6, to 8.6×10^{-4} mol, ~4, 7, and 20 nm of metal/GC nanocrystals were formed successively. These seemly indicated that lower concentration or higher dispersion of cobalt salts in reactants would produce smaller diameter of nanocrystals, and concentration of Co could determine diameter of nanocrystals. However, to know how to control thickness of carbon shells of nanocrystals, it was necessary to further study and experiment in next works.

3.2. ^{60}Co-Co/GC Nanocrystals. The ^{60}Co-$Co(NO_3)_2$ was placed into ethanol suspension of reactants and sonicated

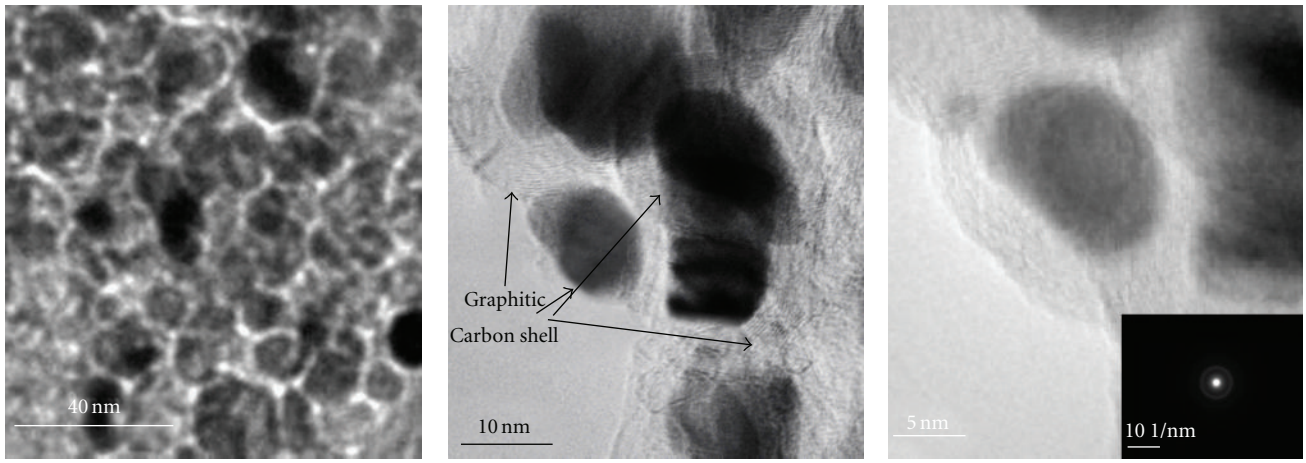

Figure 2: The TEM and HRTEM images of ^{60}Co-Co/GC nanocrystal; (a): the image of TEM ~20 nm; (b): the image of HRTEM; (c): image of HRTEM and X-ray crystallography; the core of nano Co is ~14 nm; the thickness of cover layer is ~4 nm.

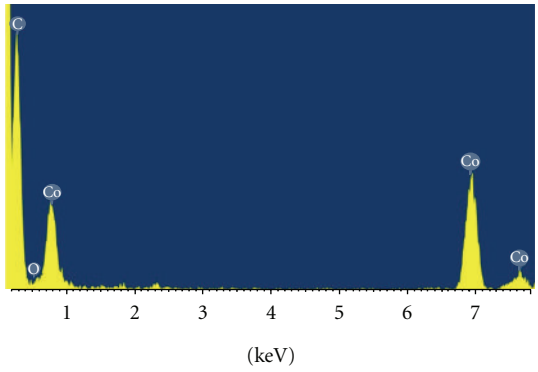

Figure 3: The energy dispersive X-ray spectrometer (EDS) of Co/GC nanocrystals, the atomic percentage of C, Co, and O are 73.77%, 25.73%, and 0.33%, respectively.

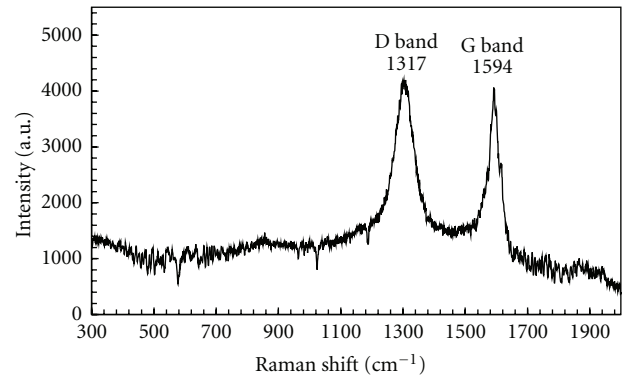

Figure 4: The Raman spectrums (excitation 785 nm)of Co/GC nanocrystals, showing the G and D bands of graphitic carbon.

it for 1 h, then ^{60}Co-Co/GC nanocrystals were prepared according to ditto method. The products were centrifugated and thoroughly washed until radioactive counts cannot be detected in supernatant. Results showed that yield of ^{60}Co-Co/GC nanocrystals was very low and less than 6%, $y = 5.77 \pm 0.23\%$ which indicted that a spot of Co, reduction production by H_2, can be embedded into graphite carbon to make Co/GC nanocrystals *via* methane CVD method. Figure 1 showed schematic diagram of a ^{60}Co/GC nanocrystal, the gamma ray can be emitted and detected by gamma counter, so it will be facilitative to quantify content of nanocrystals in tissues *in vivo*. Meanwhile, after outside graphite carbon shells of nanocrystals functionalized with chemical groups or drug molecules, the nanocrystals with gamma ray can be applied as a new radioactive imaging agent into single-photon emission computed tomography (SPECT).

3.3. Biodistribution in Mice. A mass of ^{60}Co-Co/GC nanocrystals were accumulated in lung, liver, and spleen at 1, 6, 12, 18, and 24 h, and highest accumulation in three tissues at 6 h, but low distribution in other tissues at all times. Several studies have implicated endocytosis as a cellular uptake mechanism of nanoparticles [11–13], so it was possible that ^{60}Co-Co/GC nanocrystals from blood were integrated into the phagocytic cells. As macrophages were highly concentrated in the liver and spleen, it could be possible for a large number of ^{60}Co-Co/GC nanocrystals to accumulate there. Therefore, most part of ^{60}Co-Co/GC nanocrystals were accumulated quickly in liver and spleen. The observation, along with the high-level accumulations of ^{60}Co-Co/GC nanocrystals in organs like the liver, spleen, and lungs, suggests that the rapid uptake of the nanotubes was through the mononuclear phagocytes in the reticuloendothelial system (RES) [14]. Such an uptake mechanism involving RES is consistent with the general conception on the fate of nanoparticles *in vivo* [15].

Nanocrystals began to eliminate slowly from lung and liver after 6 h, but there was a gradual increase in spleen from 12 to 24 h (Figure 4). The clearance of ^{60}Co-Co/GC

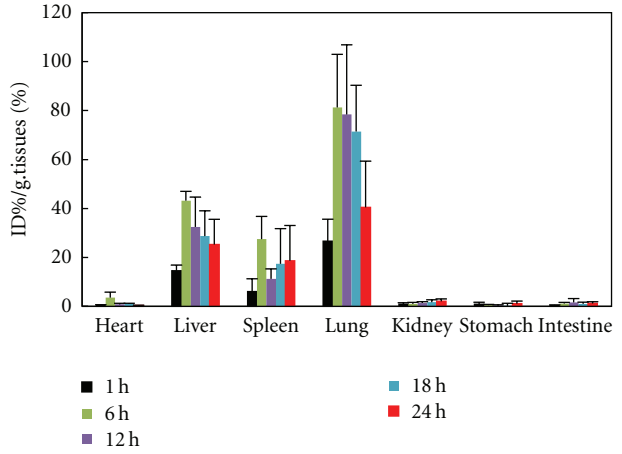

Figure 5: The biodistribution of ^{60}Co-Co/GC in different time after injection.

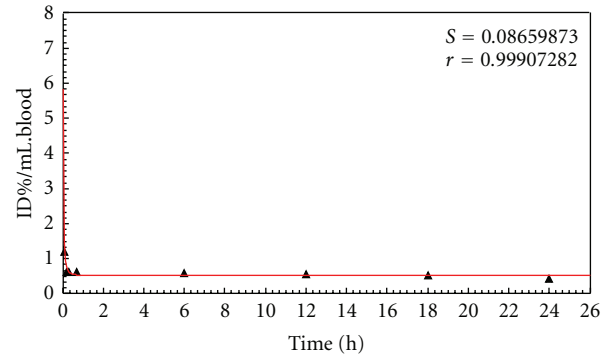

Figure 6: The time kinetic carve of ^{60}Co-Co/GC in blood after injection.

nanocrystals from the lungs may be due to two possible pathways. One is that the nanocrystals are secreted by the alveolar macrophage as mucus through mucociliary transport to leave the lungs. The other is that the interstitial nanocrystals are transferred through the lymph nodes and finally into the spleen. This seems consistent with the observed gradual increase in the uptake by the spleen over the same time period [16] (Figure 5).

The biodistribution of graphite carbon nanoparticles have been massively studied in previous works [14, 15]. It was reported that high biodistribution can be detected in liver and spleen after *i.v.* with fullerenes [14, 15]. Li et al. have studied biodistribution of $C_{60}(OH)_x$ labeled with ^{99m}Tc in mice, and established that most of ^{99m}Tc-$C_{60}(OH)_x$ can accumulated in liver, spleen, and kidney and with higher biodistribution in lung [14]. The biodistribution and metabolism of an endohedral $^{166}Ho_x@C_{82}(OH)_y$ metallofullerol were studied in BALB/c mice and Fischer rats and found that high levels of radioactivity has been localized in liver and spleen, and with negligible accumulation in the lung [15]. Compared with our results, although differential sequence of distribution in tissues was observed, basic behavior and fate of fullerene *in vivo* was similar with Co/GC nanocrystals. For some difference, it may be due to size of multilayer ^{60}Co-Co/GC nanocrystals, and further experimental verification and mechanistic elucidation are required.

3.4. Hemodynamics and Excretion Study in Blood. The hemodynamics of ^{60}Co-Co/GC nanocrystals was shown in Figure 6, the results showed that ^{60}Co-Co/GC nanocrystals can be eliminated rapidly from blood and closed to background level in 10 min. It suggested that the clearance time from blood was very short, which may be because that most part of ^{60}Co-Co/GC nanocrystals were detained rapidly in lung, liver, and spleen within short time (Figure 5).

The distribution was still higher and closed to 40, 25 and 18% ID/g in lung, liver and spleen tissues at 24 h. (Figure 5), which indicates that ^{60}Co-Co/GC nanocrystals were eliminated hardly from these tissues within 24 h. Meanwhile, few nanocrystals could be detected in blood from 10 min to 24 h, so the nanocrystals can be hardly transported to kidney so as to empty from body *via* urine (Figure 6). We conferred that lower content of blood of nanocrystals was due to high residence in lung, liver, and spleen. Therefore, a few nanocrystals would be transported to other organs, and result in lower distribution in these tissues.

Table 1: The excretion of ^{60}Co-Co/GC ($n = 6$).

Time/h	Excretion	
	Urine/%	Feces/%
0–6	1.96 ± 0.37	0.40 ± 0.04
6–12	1.06 ± 0.45	0.28 ± 0.02
12–24	3.07 ± 1.70	1.17 ± 0.71
Total	6.09 + 0.74	1.85 ± 0.23

Table 1 showed that excretion of ^{60}Co-Co/GC nanocrystals was very low in 24 h, ~1.96% of nanocrystals were excreted from body *via* urine, and just ~0.4% by feces in 6 h. Total excretion in 24 h was less than 10% *via* urine and feces.

In conclusion, most of ^{60}Co-Co/GC nanocrystals can be retained rapidly in lung, liver, and spleen for short time (Figure 5). Because few ^{60}Co-Co/GC nanocrystals can be detected in blood after 10 min (Figure 6), and then nanocrystals would be transported hardly into other tissues *via* blood circulation. So, to therapy and diagnose target-site of tumor or focus in special organization such as stomach, kidney, and intestines, it would be difficult to selectively localize using external magnetic field in human or animals *in vivo*. Our experimental results were highly consistent with distribution of pristine SWCNTs of Yang et al. [16], and they thought that the different morphology and dispersion characteristics of pristine carbon nanotubes from those of their functionalized counterparts can induce difference in distributions *in vivo*. Therefore, for unfunctionalized and pristine ^{60}Co-Co/GC nanocrystals, it would be indispensable and important to functionalize and modify with chemical method so as to change behavior and fate *in vivo*.

4. Conclusion

The larger sizes of multilayer Co/GC nanocrystals were synthesized successfully in our work; higher biodistribution were observed in lung, liver, and spleen and low biodistribution in other tissues after *i.v.* with ^{60}Co-Co/GC nanocrystals; the clearance from blood was rapid, which was due to high retention of ^{60}Co-Co/GC nanocrystals in three tissues; and the nanocrystals cannot be excreted rapidly by urine and feces from body in 24 h.

Acknowledgment

This study was conducted with financial support from National Natural Science Foundation of China (nos. 20871062, J1030932, and J0630962).

References

[1] J. M. Bai and J. P. Wang, "High-magnetic-moment core-shell-type FeCo–Au/Ag nanoparticles," *Applied Physics Letters*, vol. 87, no. 5, Article ID 152502, 2005.

[2] U. Hafeli, W. Schutt, J. Teller et al., *Scientific and Clinical Applications of Magnetic Carriers*, Plenum Press, New York, NY, USA, 1997.

[3] C. B. Murray, S. Sun, W. Gaschler, H. Doyle, T. A. Betley, and C. R. Kagan, "Colloidal synthesis of nanocrystals and nanocrystal superlattices," *IBM Journal of Research and Development*, vol. 45, no. 1, pp. 47–56, 2001.

[4] V. F. Puntes, K. M. Krishnan, and A. P. Alivisatos, "Colloidal nanocrystal shape and size control: the case of cobalt," *Science*, vol. 291, no. 5511, pp. 2115–2117, 2001.

[5] D. P. Dinega and M. G. Bawendi, "Eineaus der LosungzuganglicheneueKristallstruktur von Cobalt," *Angewandte Chemie International Edition*, vol. 111, pp. 1906–1909, 1999.

[6] A. Hütten, D. Sudfeld, I. Ennen et al., "New magnetic nanoparticles for biotechnology," *Journal of Biotechnology*, vol. 112, no. 1-2, pp. 47–63, 2004.

[7] C. Desvaux, C. Amiens, P. Fejes et al., "Multimillimetre-large superlattices of air-stable iron-cobalt nanoparticles," *Nature Materials*, vol. 4, no. 10, pp. 750–753, 2005.

[8] Z. Turgut, J. H. Scott, M. Q. Huang, S. A. Majetich, and M. E. McHenry, "Magnetic properties and ordering in C-coated Fe_xCo_{1-x} alloy nanocrystals," *Journal of Applied Physics*, vol. 83, no. 11, pp. 6468–6470, 1998.

[9] W. S. Seo, J. H. Lee, X. Sun et al., "FeCo/graphitic-shell nanocrystals as advanced magnetic-resonance-imaging and near-infrared agents," *Nature Materials*, vol. 5, no. 12, pp. 971–976, 2006.

[10] F. Tuinstra and J. L. Koenig, "Raman spectrum of graphite," *Journal of Chemical Physics*, vol. 53, no. 3, pp. 1126–1130, 1970.

[11] M. Marsh and H. T. McMahon, "The structural era of endocytosis," *Science*, vol. 285, no. 5425, pp. 215–220, 1999.

[12] S. Mukherjee, R. N. Ghosh, and F. R. Maxfield, "Endocytosis," *Physiological Reviews*, vol. 77, no. 3, pp. 759–803, 1997.

[13] P. Cherukuri, S. M. Bachilo, S. H. Litovsky, and R. B. Weisman, "Near-infrared fluorescence microscopy of single-walled carbon nanotubes in phagocytic cells," *Journal of the American Chemical Society*, vol. 126, no. 48, pp. 15638–15639, 2004.

[14] Q. N. Li, Y. Xiu, X. D. Zhang et al., "Preparation of ^{99m}Tc – $C_{60}(OH)_x$ and its biodistribution studies," *Nuclear Medicine and Biology*, vol. 29, no. 6, pp. 707–710, 2002.

[15] D. W. Cagle, S. J. Kennel, S. Mirzadeh, J. M. Alford, and L. J. Wilson, "In vivo studies of fullerene-based materials using endohedral metallofullerene radiotracers," *Proceedings of the National Academy of Sciences of the United States of America*, vol. 96, no. 9, pp. 5182–5187, 1999.

[16] S. T. Yang, W. Guo, Y. Lin et al., "Biodistribution of pristine single-walled carbon nanotubes in vivo," *Journal of Physical Chemistry C*, vol. 111, no. 48, pp. 17761–17764, 2007.